

# Digital-Twin-Enabled 6G Mobile Network Video Streaming Using Mobile Crowdsourcing

Lianyong Qi, Xiaolong Xu, *Member, IEEE*, Xiaotong Wu, Qiang Ni, *Senior Member, IEEE*, Yuan Yuan, Xuyun Zhang

**Abstract**—Digital-twin-enabled cloud-centric architecture is a promising evolution trend of sixth generation (6G) network, which brings new opportunities and challenges for mobile video streaming-related services requiring the exponentially increasing traffic demands. Device-to-Device (D2D) communication paradigm is an attractive technique to alleviate the problem. However, the previous research work on D2D built on individuals' random mobility or position snapshot and cannot guarantee the stable communication flow. In this paper, we leverage the cybertwin as a centric controller and take advantages of crowdsourcing technology to attract mobile users to follow the specified path and share their network resources with other users. The design of the specified path is formulated as a problem of user recruitment optimization with cost constraint, which is a NP-Hard problem. Firstly, we investigate a special case of only one mobile user to offer the network resource and present a pseudo-polynomial time algorithm. Secondly, we present a graph-partition-based approach to solve the more complex case of multiple mobile users. Thirdly, we discuss the least expected budget to achieve the maximum utility in an ideal model. Fourthly, we perform extensive experiments to evaluate and compare the performance with the typical ones in simulated digital-twin-enabled 6G networks.

**Index Terms**—Digital twin, video streaming, mobile crowdsourcing, communication assistance, movement optimization.

## I. INTRODUCTION

WHEN fifth generation (5G) network is gradually put into commercial use all over the world, some researchers in academia and industry are investigating the potential technical routes of the next generation 6G network [1]–[5]. For instance, Yu et al. [6] proposed a novel 6G network paradigm named digital-twin-enabled cloud-centric network architecture. As shown in Fig. 1, cybertwin is an important digital-twin component of the end in the virtual cyberspace of edge cloud [3], [4]. Its most significant function

L. Qi is with College of Computer Science and Technology, China University of Petroleum (East China) and School of Computer Science, Qufu Normal University, China. E-mail: 20220115@upc.edu.cn.

X. Xu is with School of Software, Nanjing University of Information Science and Technology, China. E-mail: xlxu@ieee.org.

X. Wu is with School of Computer and Electronic Information, Nanjing Normal University, China. Email: wuxiaotong@njnu.edu.cn

Q. Ni is with School of Computing & Communications, Lancaster University, UK. E-mail: q.ni@lancaster.ac.uk

Y. Yuan is with School of Computer Science and Engineering, Beihang University, and State Key Laboratory of Software Development Environment, and Zhongguancun Laboratory, China. Email: yuan21@buaa.edu.cn

X. Zhang is with Department of Computing, Macquarie University, Australia. Email: xuyun.zhang@mq.edu.au

Manuscript received April 19, 2005; revised August 26, 2015.  
(Corresponding Author: Xiaolong Xu)

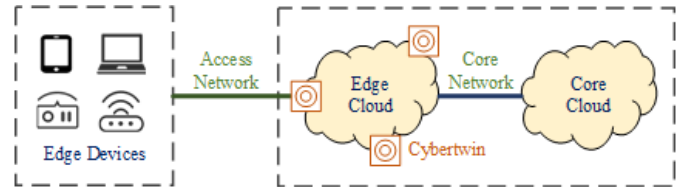


Fig. 1. An architecture of digital-twin-enabled cloud-centric 6G network.

is communication assistant, i.e., collecting the requesters from users' devices and then offering the corresponding services deployed in edge cloud. Not only that, it also supports other functions, including network behavior logger, digital asset owner and so on. As a result, the paradigm brings a series of new opportunities and challenges for network architectures and services, especially in mobile domain.

In recent years, mobile video streaming services deployed in smart devices have attracted more and more users and brought significant economic benefits. According to recent reports [7], online videos have accounted for more than half of mobile network traffic. Mobile users utilize smart devices to conveniently watch various kinds of high-quality videos related to education, health, sports and so on. In addition, some effective techniques (e.g., virtual reality (VR) [8], augmented reality (AR) [9]) and novel funny platforms (e.g., cloud game [10]) greatly extend the application of mobile videos. However, these video streaming applications and services generate high network traffic and cause greater pressure on mobile networks. As a result, it is possible to lead to a decline of quality of service (QoS) and quality of experience (QoE) in mobile video streaming-related applications [11].

Naturally, there is a fundamental question about *how to implement mobile video streaming-related services with low delay and high quality for edge devices under digital-twin-enabled 6G network*. Combined with the specific architecture of 6G network shown in Fig. 1, we derive the following properties to investigate the difficulties: (§1) the primary bottleneck to limit transmission speed is the network between edge devices and cybertwin, i.e., access network; (§2) cybertwin knows service requests from its connected edge devices and thus could control their communication to optimize users' quality of service, especially for network delay [6]; and (§3) the difference of network performance among edge devices is very huge. Therefore, it is important to leverage the control role of cybertwin (i.e., §2) and adopt proper techniques to reduce the delay of those devices with poor network performance

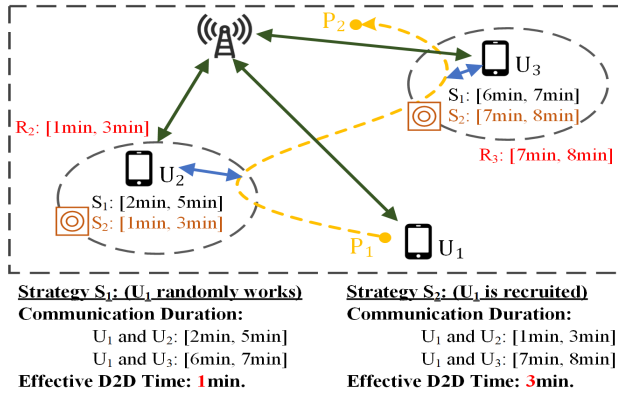


Fig. 2. Motivation example: Two strategies for mobile video streaming enhancement by D2D communication in digital-twin-enabled 6G networks.

to the access network (i.e., §1 and §3).

Faced with the development of mobile video streaming, Device-to-Device (D2D) communication paradigm is an attractive technology to alleviate the problem [12]–[16]. The advanced paradigm helps mobile devices communicate with each other in cellular networks with no need of a base station or a core network and can greatly improve spectral efficiency and reduce delay [17]. Thus, the advanced technology is expected to implement video streaming enhancement, i.e., reducing the delay of edge devices with poor access network in digital-twin-enabled 6G by leveraging the strong network ability of the others. However, the previous research work on D2D usually built on individuals' random mobility or position snapshot, implying that it is hard to guarantee the stable communication flow and is thus not well suited for video streaming transmission in 6G networks. To this end, it is worthwhile trying to improve the advanced paradigm for some video streaming-related services and applications (e.g., cloud game, AR, and VR).

To this end, we investigate *D2D communication-based mobile video streaming enhancement (VSE) for edge devices with poor network performance in digital-twin-enabled 6G network*. We find that leveraging the crowdsourcing technology to guide users' movement under the control of the cybertwin is helpful in improving the performance of D2D communication. We take Fig. 2 as a simple example to show our research motivation. There are three smartphone users, i.e.,  $U_1$ ,  $U_2$ , and  $U_3$ . The VSE request time range of User  $U_2$  is [1, 3], while the VSE request time range of User  $U_3$  is [7, 8]. User  $U_1$  is moving from Position  $P_1$  to  $P_2$  and offers the VSE service by his smart device. There are two different VSE strategies, i.e.,  $S_1$  and  $S_2$ , that have different paths. In  $S_1$  without a control of cybertwin,  $U_1$  randomly walks from  $P_1$  to  $P_2$ . In this case, User  $U_1$  offers the service time of one minute to User  $U_2$  and  $U_3$ . In  $S_2$ , the cybertwin guides  $U_1$  through the specified path. Meanwhile, the service time of  $U_1$  increases from one minute to three minutes. Therefore, it is demonstrated that mobile users' movement controlled by the cybertwin (i.e.,  $S_2$ ) efficiently improves the performance of D2D communication technology, so as to enhance the quality of mobile video streaming-related services.

The above finding inspires us to analyze how to design the

optimal paths of mobile users to maximize the communication efficiency in digital-twin-enabled 6G network and enhance the quality of mobile video-related services. Actually, the pioneering work [18]–[21] has indicated that the moving paths of mobile users can be guided by a controller with the proper incentive schemes to share the network resources and thus improve the communication efficiency. However, there are three key challenges to implement optimal paths of mobile users for video service enhancement. Firstly, it is hard to quantitatively analyze the situation of the current networks and their influence on mobile video-related services and applications. Secondly, mobile users have the personalized requests with different request time, which increases the difficulty to implement the optimal design of multiple recruited users' paths. Thirdly, when there are a huge number of users and VSE requests, the computational complexity to select the proper recruited users and the design of mobile paths and the corresponding incentives is relatively high.

In response to the challenges mentioned above, we first construct a system model to utilize the centric control of cybertwin to implement video streaming enhancement in digital-twin-enabled 6G networks. Then, we formulate a problem of user recruitment optimization with cost constraints, and discuss its computational complexity. We design two efficient approaches to solve two different cases, including only one recruited mobile user and multiple mobile users. In summary, the key contributions of this paper are listed as follows:

- We construct a system model to support video streaming enhancement for those mobile services with high traffic demand in a digital-twin-enabled 6G network. By leveraging the centric control of cybertwin, it encourages edge devices to share their idle or extra resources and get a certain reward from the other devices with poor network performance. Based on the system model, it efficiently overcomes the bottleneck of the access network between edge devices and cybertwin to reduce the network delay.
- We formulate the cost-constrained user recruitment problem and demonstrate a NP-Hard problem. We investigate a special case of only one mobile user to offer the network resource and present a pseudo-polynomial time algorithm. We also present a graph-partition-based approach to solve the more complex case of multiple mobile users.
- We perform extensive experiments to evaluate the performance of the proposed algorithms under different parameter settings and compare them with the typical ones. Experimental results show that the proposed algorithms successfully integrate D2D communication with mobile live video enhancement and offer the high QoS and QoE for mobile video-related services.

The remaining part of the paper is organized as follows. Section II introduces the recent works about digital-twin-enabled 6G networks and D2D communication. Section III evaluates the throughput measurement of the current network. Section IV constructs a system model and formulates a recruitment optimization problem. Section V and Section VI analyze the optimization problem in two cases of only one recruited user and multiple users, respectively. Section VII

provides some practical discussions. Section VIII evaluates the proposed algorithms. Section IX concludes the paper.

## II. RELATED WORK

### A. Digital-Twin-Enabled 6G Network for Video Streaming

When 5G network is continuously deployed around the world, some researchers in academia and industry are exploring the possible technology directions of the next-generation network [1]–[5]. Tang et al. [1] investigated the possibility of utilizing the intelligent analysis technologies (e.g., predictive classification, speech recognition) to implement a digital-twin-enabled 6G vehicular network with high security and rapid response. Xu et al. [3] implemented a cybertwin-based 6G networks based on deep reinforcement learning, which greatly improved the communication performance. Lu et al. [4] proposed a distributed deep learning architecture over the digital twin-based 6G networks and utilized blockchain technology to enhance its ability in multiple aspects, such as privacy, security, efficiency, and utility. Hazra et al. [5] proposed a 6G-aware network model based on fog computing, which dispatches the resources of service providers and offers demand specific services to users. Meanwhile, the model implemented the revenue maximization of service providers and users' service delay and price minimum.

In recent years, there have been some research works to design proper mechanisms with high QoS and QoE of wireless multimedia applications in digital-twin-enabled 6G network, against some constraints, such as energy consumption [22], communication delay [23]–[26]. Sodhro et al. [22] designed artificial intelligence-based 6G networks to improve energy efficiency and quality of experience when users are enjoying the multimedia services. Zhang et al. [23] solved a special problem of delay violation probability minimization to derive the closed-form solution of the optimal rate adaptation policy for each mobile user over 6G cell-free massive multi-input multi-output mobile wireless networks in the finite blocklength regime. Overall, the novel network paradigm brings the new opportunities and challenges for communication management of video streaming-related services with the high requirement of network demand [27], [28]. Meanwhile, the related research on QoS and QoE improvement of multimedia applications in 6G networks is still at an initial stage.

### B. D2D communication for Video Streaming

As an efficient communication technology, device-to-device communication implements the cooperation of a lot of smart devices with each other to improve the network utilization [14]–[16]. In the beginning, D2D communication was proposed to implement multi-hop relays in cellular networks [29]. Subsequently, D2D communication was introduced into multiple applications and services, such as spectral efficiency improvement [29], cellular offloading [30], and video dissemination [31]. For instance, Cao et al. [32] utilized D2D communication to propose a social-aware video multicast framework that designed a unique video encoding structure to get missing video packets and thus enhanced the quality of video-related applications. Liu et al. [33] combined deep

learning approaches to develop an active video content caching mechanism over a recommendation system and consistent hash for D2D communication, which minimizes the transmission delay and maximizes the hitting probability.

In addition, D2D communication is widely applied to video dissemination. Golrezaei et al. [34] presented a novel architecture for wireless video dissemination, in which wireless terminals are viewed as caching helpers and distribute video via D2D communications. Zhang et al. [35] combined social relationships and physical conditions among mobile users and utilized D2D communication for cooperative video dissemination. Yan et al. [36] proposed a low complexity centralized algorithm based on network coding mechanisms in D2D communications to implement the fast video dissemination, thereby improving the quality of service of real-time scalable video applications. Wu et al. [37] leveraged D2D communications and designed a user-centric video communication approach helping a number of users cooperate with each other to cache and share videos with each other.

Although D2D communication is conducive to network optimization of mobile video-related applications, the above research works always require that mobile users cache and share video clips [31]. It greatly increases the D2D communication delay for the video-related applications and is not well suited to the live video services with the requirement of low delay (e.g., cloud game [10], VR [8], and AR [9]). Faced with the challenge, we introduce the crowdsourcing technology to improve the quality of the services. Existing integration of videos and crowdsourcing paradigm focused on video generation [38], and video delivery [39]. In this paper, we investigate the problem to design the reasonable movement path and provide the corresponding incentive for the mobile users to improve the whole system's D2D communication efficiency in a digital-twin-enabled 6G network.

## III. 4G THROUGHPUT MEASUREMENT STUDY

### A. 4G/LTE Network Throughput Measurement Study

We introduce and analyze the actual situation of various applications under the practical network in Ghent, Belgium [40]. While performing the bandwidth measurement, different transportation conditions are taken into consideration. The data consist of throughput logs under six cases, such as bicycle, bus, car, foot, train, and tram. The corresponding mean values and deviations are shown in Table I. From Table I, we observe that the 4G throughput for each individual is high as a whole compared to common low individual 3G throughput [41] and even in the train scene, the individual 4G throughput has a mean value of 22.7Mbps. Moreover, in all these scenes, individual 4G throughput shows high volatility indicated by

TABLE I  
MEAN VALUE AND STANDARD DEVIATION OF 4G/LTE BANDWIDTH LOGS.

Scene (Mbps)	Bicycle	Bus	Car	Foot	Train	Tram
Mean Value	28.2	31.9	33.9	28.2	22.7	29.2
Std. Dev.	15.2	17.3	15.8	16.0	14.6	17.3

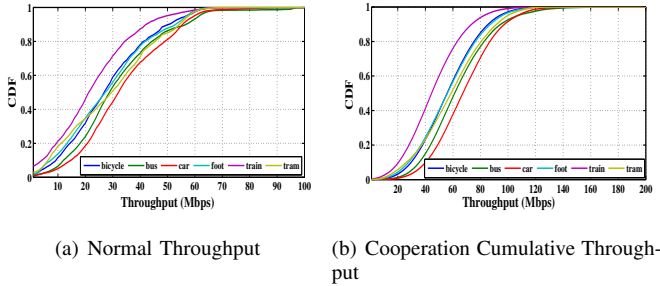


Fig. 3. The cumulative distribution function (CDF) in six cases.

the high deviation value and turns to be vulnerable to environmental influences, such as weather, transportation routes, transportation types. Actually, one individual's throughput has a large span from 0Mbps to 100Mbps. Fig. 3(a) shows the cumulative distribution function of one individual's throughput in six scenes. All these throughput logs reflect the possible common conclusion. That is, one individual's throughput is highly dynamic depending on user mobility, weather, building shields, congestion, etc.

### B. Further Quantitative Analysis

For the dynamic characteristic, we leverage a probabilistic quantitative analysis to study the effect of individual dynamic throughput and then analyse the cooperation's influence, i.e., real-time D2D communication, on the improvement of online video.

1) *Online video watching without D2D communication:* We investigate two classes of video applications, including 4K video and FHD, by taking current smartphone market status into consideration<sup>1</sup>. In general, when a nominal bitrate is up to 5.2Mbps, the users can enjoy a high quality service for a FHD 1080p video. When a nominal bitrate is up to 21.4Mbps, the users can enjoy a high quality service for a 4K 2160p video. Table II shows the concrete results of the fluent playback probabilities of two classes of video applications under the practical 4G network. It is obvious to find that the common 4G network is able to offer the low delay for FHD video, while the delay of 4K video is relatively high. In the worst case (i.e., the train), the fluent playback probability of 4K video is less than 50%.

**Observation 1:** The common 4G network can guarantee the good fluent playback of online FHD video. However, the corresponding guarantee is impossible for 4K video.

2) *Online video watching in support of real-time D2D communication:* With the help of real-time D2D communication, the fluent playback probability is obviously increasing as the number of mobile users increases, which is shown in PROPOSITION 1. PROPOSITION 1 shows that one mobile user's fluent playback probability is improved exponentially with the increase of mobile users.

**Proposition 1:** Assume that the 4G network bandwidth of mobile users are independent identically distributed with CDF

<sup>1</sup>For convenience and portability, a smartphone's screen usually has a limited size with different resolutions. The videos with 1080p or a little higher definition can currently allow mobile users to enjoy the best view experience.

TABLE II  
FLUENT PLAYBACK PROBABILITY OF TWO CLASSES OF VIDEOS  
THROUGH DIFFERENT 4G/LTE BANDWIDTH CONFIGURATIONS.

Video	Conf.	Bicycle	Bus	Car	Foot	Train	Tram
FHD	1x	0.9470	0.9733	0.9746	0.9256	<b>0.8853</b>	0.9259
	2x	0.9983	0.9995	0.9995	0.9974	<b>0.9891</b>	0.9964
4K	1x	0.6409	0.7220	0.7862	0.6182	<b>0.4941</b>	0.6345
	2x	0.9581	0.9824	0.9891	0.9446	<b>0.8830</b>	0.9297

of  $F$ . When there are  $z$  users, the CDF (denote as  $G$ ) of the total available network bandwidths satisfies the following equation:

$$G(x) \leq F^z(x). \quad (1)$$

*Proof:* When there are two mobile users, we have

$$G(x) = \int_0^x \int_0^{x-t} f(y)f(t)dydt \leq \left( \int_0^x f(t)dt \right)^2 = F^2(x).$$

Then, an iteration process on users' number can complete the proof. ■

From PROPOSITION 1, given any demand  $x_0$ , we have  $1 - G(x_0) \geq 1 - F^z(x_0)$ . Based on the finding, when the D2D communication is built among  $z - 1$  users and some mobile user, it can help the user efficiently improve the fluent playback of video-related applications. Meanwhile, since the interface of some smart device is limited, it is impossible to support all the users to construct D2D communication with the user. As a result, it is reasonable to consider a common case, in which two mobile users connect their smart devices with each other via Wi-Fi Direct. We implement the quantitative analysis to evaluate the fluent playback probability of some mobile user in the support of the mobile device of another user. Fig. 3(b) shows the detailed CDF of the network bandwidth that the smart device is able to use. Table II shows the impact of the support of D2D communication on the video-related applications. It is obvious to find that under the support of D2D communication, the fluent playback probability of 4K video has an increase of more than 90 percent. In addition, the fluent playback probability of FHD video has the significant increase in different cases. Therefore, we present the following observation to illustrate the function of the cooperation of multiple users.

**Observation 2:** The real-time D2D communication among several mobile devices can be conducive to the significant increase of the fluent playback probability of video-related applications, such as FHD and 4k video.

Based on OBSERVATION 1 and 2, we derive that the real-time D2D communication built by several mobile devices can efficiently help some mobile user enjoy the better QoS and QoE of online video-related applications.

## IV. MOBILE VIDEO STREAMING ENHANCEMENT IN DIGITAL-TWIN-ENABLED 6G NETWORK

### A. System Model

In a digital-twin-enabled 6G network, the core component, i.e., cybertwin, connects a large number of mobile devices



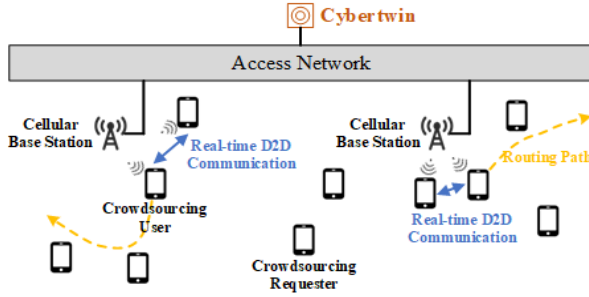


Fig. 4. The problem scenario where smartphone users enjoy the VSE services with support of recruited mobile users in a digital-twin-enabled 6G network.

via access network and supports the communication assistant. That is, it collects the requests from mobile users' devices and then offers the corresponding services from the third party. Combined with the crowdsourcing and D2D communication, cybertwin can be as a guide to recruit mobile users with redundant network resources and enhance the QoE and QoS of mobile video-related applications. The concrete scenario is shown in Fig. 4. Suppose that there is a region  $\Lambda$  in which a lot of mobile users enjoy video-related services on smart devices. The region  $\Lambda = \{1, 2, \dots, K\}$  is made up of  $K$  smaller regions that are non-overlap and have equal areas. At some point in time  $T$ , there are  $I$  crowdsourcing requesters that need the VSE service and  $J$  crowdsourcing users that offer the corresponding service via D2D communication technology. After some crowdsourcing users receive and support the request, the crowdsourcing requester is able to enjoy the high QoS video-related services via an access network. Meanwhile, the location of crowdsourcing requester  $i$  is defined as  $d_i$ . Suppose that the VSE service area  $S_{j,k}$  that each crowdsourcing user  $j$  supports is equal to the region  $k \in \Lambda$  that he is located at, i.e.,  $S_{j,k} = \{k\}$ .

In this model, there is an important guide role, i.e., cybertwin, which is defined as  $\mathcal{R}$ . Cybertwin  $\mathcal{R}$  knows the communication information of its connected edge devices and could be a controller to execute the corresponding actions for different participants. That is, after receiving some incentive measures provided by the cybertwin  $\mathcal{R}$  [18], [19], the crowdsourcing user moves from his current location to the destination that cybertwin requires and offers the VSE service to the crowdsourcing requester. As a result, the service range of crowdsourcing users are expanded to improve the whole network utilization.  $\mathbf{P} \in \mathbf{R}^{k \times k}$  is defined as a cost matrix, in which any element  $p_{k_1, k_2}$  represents the moving cost between any two regions  $(k_1, k_2)$ . In particular, when  $k_1 = k_2$ , we have  $p_{k_1, k_2} = 0$ . More importantly, the cost matrix has the following property:

$$p_{k_1, k_2} \leq p_{k_1, k_3} + p_{k_3, k_2}, \quad \forall k_1, k_2, k_3 \in \Lambda. \quad (2)$$

It is important to note that the crowdsourcing user who is supporting the VSE service should be located at the specified region. Meanwhile, the crowdsourcing users should move according to the *homogenous-constant-speed* mobility requirement. In detail, *homogeneity* represents that all crowdsourcing users move simultaneously from a region to any specified

destination and *constant-speed* implies that the transfer time of any crowdsourcing user should satisfy the triangle inequality. To this end,  $\mathbf{Q} \in \mathbf{R}^{k \times k}$  is defined as a time matrix, in which any element  $q_{k_1, k_2}$  refers to the transfer time between any two regions  $(k_1, k_2)$ . In particular, when  $k_1 = k_2$ , we have  $q_{k_1, k_2} = 0$ . Meanwhile, the following triangle inequality holds:

$$q_{k_1, k_2} \leq q_{k_1, k_3} + q_{k_3, k_2}, \quad \forall k_1, k_2, k_3 \in \Lambda. \quad (3)$$

In a digital-twin-enabled 6G network, cybertwin  $\mathcal{R}$  undertakes a control function to guide the moving paths of the crowdsourcing users and optimize the performance of the whole network. As described in [6], the cybertwin first collects the regions that all the mobile users are located at and then formulates the paths of crowdsourcing users for the requests from crowdsourcing requesters. Specifically, the controller computes which region any crowdsourcing user should move to at different times and determines which crowdsourcing requester any crowdsourcing user should serve via a real-time D2D communication through the access network according to some rules or objectives (such as utility maximum).

### B. Problem Formulation

As a central controller in the digital-twin-enabled 6G network, cybertwin  $\mathcal{R}$  needs to solve an optimization problem.  $s_i$  and  $e_i$  are the starting and termination time of any crowdsourcing requester  $i$  that wants the VSE service, respectively.  $a_{t,j} \in \{0, 1\}$  is defined as whether or not crowdsourcing user  $j$  is moving at some point  $t$  in time.  $y_{t,j}^i \in \{0, 1\}$  is defined as whether or not the crowdsourcing request of mobile user  $i$  is finished by crowdsourcing user  $j$  at some point  $t$  in time. For simplicity, at some point  $t$  in time, a crowdsourcing user just supports only one the VSE service request of a mobile user through the access network.  $y_t^i = \sum_j y_{t,j}^i \in \{0, 1\}$  refers to whether the VSE service request of crowdsourcing requester  $i$  is finished by the recruited crowdsourcing users  $\{j\}$  at some point  $t$  in time. In the following, the utility of some crowdsourcing requester and the utility of the whole system are formally defined.

**Definition 1 (Requester Utility):** The utility  $U_i$  of some crowdsourcing requester  $i$  is denoted as the time intervals of the VSE service that crowdsourcing users support and is calculated as  $U_i = |\{t | y_t^i = 1\}|$ .

From this definition, one requester's utility metric has a linear positive correlation with real-time D2D communication time enjoyed.

**Definition 2 (System Utility):** The utility of the system in a digital-twin-enabled 6G network is denoted as the total utilities of all the crowdsourcing requesters and is calculated as  $U = \sum_i U_i$ .

$l^j$  is defined as the moving path of crowdsourcing user  $j$  and consists of multiple regions, in which  $l_t^j$  is the position of crowdsourcing user  $j$  at some point  $t$  in time. In special,  $l_0^j$  is the starting region of crowdsourcing user  $j$ .  $\mathcal{C}(j \xrightarrow{t} l^j)$  is defined as the cost of crowdsourcing user  $j$  under the moving path  $l^j$  at some point  $t$  in time and is calculated as

$$\mathcal{C}(j \xrightarrow{t} l^j) = \begin{cases} 0, & t = 0 \\ \mathcal{C}(j \xrightarrow{b(t)} l^j) + p_{l_{b(t)}^j, l_t^j}, & t > 0 \end{cases} \quad (4)$$

in which  $b(t) = t^-$  refers to the last time point before  $t$ .

Based on the above definitions, the objective of recruiting crowdsourcing users is to maximize the utility  $U$  of the whole system. Meanwhile, the utility of the system is constrained by the budget that the cybertwin can offer. In general, the higher budget implies the better utility of the whole system. Therefore, we focus on the optimization problem with cost constraints that the cybertwin  $\mathcal{R}$  needs to solve and is defined as follows:

**Definition 3 (User Recruitment Optimization with Cost Constraints):** The crowdsourcing user recruitment problem (CURP) is to maximize the utility of the whole system constrained by a certain amount of budget and the moving paths of crowdsourcing users, i.e.,

$$\max_{l, y} U \quad (5)$$

$$s. t. \quad \sum_j \mathcal{C}(j \xrightarrow{T} l^j) \leq C, \quad (6)$$

$$\sum_i y_{tj}^i \leq 1, \quad \forall t, j \quad (7)$$

$$y_{tj}^i \leq 1 - a_{tj}, \quad \forall t, j, i \quad (8)$$

$$y_{tj}^i = 0, \quad \forall d_i \notin S_{j, l^j} \quad (9)$$

$$y_{tj}^i, a_{tj} \in \{0, 1\}, \quad \forall t, j, i \quad (10)$$

in which  $l = \{l^j | \forall j\}$ ,  $y = \{y_{tj}^i | \forall t, j, i\}$ , and  $C$  is the maximum budget of all the crowdsourcing users in the whole system.

In the user recruitment optimization with cost constraints, Eq. (6) determines the upper bound  $C$  of the cost budget in the whole system that is a constant value to determine the maximum utility of the whole system. Eq. (7) ensures that every crowdsourcing user only supports the request from a crowdsourcing user at some time point. Eq. (8) requires that all crowdsourcing users not support the VSE service when they are moving. Eq. (9) determines the condition of utilizing real-time D2D communication, in which the crowdsourcing requester and user should be close enough.

### C. Computational Complexity

**Theorem 1:** The Cost-Constrained User Recruitment Problem is NP-hard.

*Proof:* We attempt to demonstrate that the user recruitment problem with cost constraints is a variant of the knapsack Problem in polynomial time. We first present an example of knapsack Problem is defined as . Assume that there are a group of items  $\{1, 2, \dots, M\}$  and each item has a pair of weight and value  $(w_m, v_m)$ . The knapsack Problem is defined as

$$\max \sum_m v_m x_m, \quad s. t., \quad \sum_m w_m x_m \leq W; x_m \in \{0, 1\}, \quad (11)$$

in which  $W$  is the upper bound of the weight.

For simplicity, suppose that there are a crowdsourcing user and multiple crowdsourcing requesters in the user recruitment problem with cost constraints, i.e.,  $I = M$  and  $J = 1$ . Meanwhile, the regions that crowdsourcing requesters are in do not overlap. The enhanced intervals of crowdsourcing requesters should satisfy  $e_i + q_{max} \leq s_{i+1}, \forall i = 1, \dots, M - 1$

in which  $q_{max}$  is the maximum item in matrix  $\mathbf{Q}$ . Therefore, we have the important properties, including  $p_{k, d_i} = w_i$  for matrix  $\mathbf{P}$ ,  $e_i - s_i = v_i$ ,  $K = I + 1$ ,  $l_0^1$ , and  $C = W$ .

The moving path of crowdsourcing users is viewed as a decision problem of node selection. It is worthwhile noting that the above properties still satisfy the moving cost triangle inequality. The reason is that for any three regions  $k_1, k_2, k_3$ , we have  $p_{k_1, k_2} + p_{k_2, k_3} = w_{k_2} + w_{k_3} \geq w_{k_3} = p_{k_1, k_3}$ .  $x_i \in \{0, 1\}$  is defined as whether or not the crowdsourcing requester  $i$  supports the VSE service. The simple case of the user recruitment problem with cost constraints is similar to an example of the Knapsack Problem. Thus, the user recruitment problem with cost constraints has the same computational complexity with the Knapsack Problem, i.e., NP-hard. ■

### V. OPTIMAL RECRUITMENT ALGORITHM WITH ONE CROWDSOURCING USER

Since the computational complexity of the user recruitment problem with cost constraints is NP-hard, it is hard to design an optimal solution with  $l, y, t \in [0, T]$  in polynomial time. Here, we discuss a simple case of CURP where there is only one crowdsourcing user that offers the VSE service via D2D communication. In order to get the optimal solution, we present a meaning finding of the CURP as follows, which is conducive to reducing the number of decision variables.

**Proposition 2:** In the case of only one crowdsourcing user, the user recruitment problem with cost constraints has an optimal decision  $\Gamma^*$ . The corresponding condition is that for each crowdsourcing requester  $i$ ,  $\exists \tau_i \in [s_i, e_i]$ , it should satisfy  $y_t^i = 0, \forall t \in [s_i, \tau_i]$  and  $y_t^i = 1, \forall t \in [\tau_i, e_i]$ .

*Proof:* In order to demonstrate the proposition, it first should prove that for any *optimal* decision  $\Gamma$ ,  $\Gamma^*$  can be derived in the case of no addition of budget cost. In general, there are two common cases of  $\Gamma$ , which are listed as follows:

- **Case 1.** The crowdsourcing requester  $i$  does not get the VSE service from the crowdsourcing user. Therefore, we have  $\tau_i = e_i$ .
- **Case 2.** The starting time of crowdsourcing requester  $i$ 's VSE service offered by the crowdsourcing user is  $t_0 \in [s_i, e_i]$ . Assume that in  $\Gamma$ ,  $l_1 : [t_0, t_1]$ ,  $l_2 : [t_2, t_3]$ ,  $\dots$  are the pairs of the regions and time intervals of the crowdsourcing user.

**Adjusted Policy  $\Gamma'$ .** The time intervals that the crowdsourcing users offer the VSE service to crowdsourcing requester  $i$  is  $[t_0, e_i]$ . Then, the crowdsourcing user moves to other regions according the order of  $\Gamma$  and can not continue to support the crowdsourcing requester until it is up to the temporal-spatial coincident point. Next, the crowdsourcing user continue to offer the VSE service according to the strategy of  $\Gamma$ .

Fig. 5 shows the comparison between  $\Gamma$  and the adjusted policy  $\Gamma'$ . In order to implement the comparison, it is important to analyze the time range  $[t_0, t_c]$  where  $t_c$  is the temporal-spatial coincident point. In the time range  $[t_0, t_c]$ , the crowdsourcing user is moving to the specified regions according the same strategy of  $\Gamma$  and  $\Gamma'$ . The corresponding cost and the time  $\Delta t_f$  in  $\Gamma'$  and  $\Gamma$  are equal, respectively. Meanwhile, the utility of the whole system in the adjusted

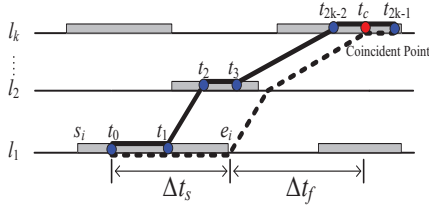


Fig. 5. The comparison between the optimal strategy  $\Gamma$  (solid line) and the adjusted policy (dotted line) used to prove **Proposition 2**.

policy  $\Gamma'$  is  $\Delta t_s = e_i - t_0 = t_c - t_0 - \Delta t_f$ . The utility of the whole system in  $\Gamma$  is equal to or less than  $\Delta t_s$  in  $\Gamma'$  and depends on whether or not the crowdsourcing user supports the VSE service in some fixed region. In other words, the adjusted policy will not reduce the utility of the whole system without the extra cost. As a result,  $\Gamma'$  is well suited to every VSE request of  $\Gamma$ . At last, according to the above discussion,  $\Gamma$  can be adjusted to the strategy of the adjusted policy with  $\tau_i = t_0$ . ■

From **Proposition 2**, once some crowdsourcing user starts providing the VSE service to some crowdsourcing requester at some region, he should finish it and then leave the region. In other words, the region that the crowdsourcing user is located at can change only when he does not offer the VSE service. The finding contributes to the design of an optimal algorithm to solve the user recruitment problem with cost constraints. We use a virtual request  $v_0$  with  $s_{v_0} = e_{v_0} = 0$  that represents the initial region of the crowdsourcing user. Then, the system sorts the requests from all the crowdsourcing requesters according to the arrival time.  $\mathcal{V} = \{v_0, v_1, \dots, v_I\}$  is defined as the group of sorted requests. The corresponding ending time should satisfy  $e_0 \leq e_1 \leq \dots \leq e_I$ .  $\Phi_i$  is defined as the group of requests which should satisfy that the sum of the completion time and the moving time should be less than  $v_i$ 's completion time. In detail, we get  $\Phi_i = \{v_j | e_j + q_{ji} \leq e_i, j = 0, 1, \dots, I\}$  and  $\Phi_0 = \{v_0\}$ . Since **Proposition 2** indicates that some crowdsourcing user responds to and completes a request,  $\Phi_i$  consists of the possible requests before the time point of  $v_i$ .

According to the above discussion, the optimal utility of the whole system can be computed as follows:

$$U[i][c] = \begin{cases} -\infty, & c < 0 \text{ or } v_0 \notin \Phi_i \\ 0, & i = 0, c \geq 0 \\ \max_{j \in \Phi_i \setminus \{i\}} U[j][c_{ji}] + u_{ji}, & i \geq 1, c \geq 0 \end{cases} \quad (12)$$

in which  $c$  is the upper bound of the cost,  $u_{ji} = e_i - \max\{s_i, e_j + q_{ji}\}$ ,  $c_{ji} = c - p_{ji}$ ,  $p_{ji}$  is the transfer cost between  $v_j$ 's and  $v_i$ 's regions. Eq. (12) presents the concrete result of  $U[i][c]$  under different cases. When the total cost is less than 0,  $U[i][c]$  is negative and can not be accepted by the crowdsourcing users. When  $\Phi_i \not\supset \{v_0\}$ , the crowdsourcing user does not arrive at the specified region in time and can not offer the VSE service. When the crowdsourcing users can not offer the VSE service, his corresponding utility is  $U[i][c] = -\infty$ . On the other hand, when  $c \geq 0$  and  $\Phi_i \supset \{v_0\}$ ,  $U[i][c]$  depends on all previous one sub-problems, i.e.,  $U[j][c - p_{ji}]$ ,  $j \in \Phi_i$ .

### Algorithm 1 Optimal Path Scheduling Algorithm

**Input:** Cost matrix  $\mathbf{P}$ , Time matrix  $\mathbf{Q}$ , a set of sorted requests  $v_i, i \in \{I\}$ ;

**Output:** Decision variables  $\mathbf{l}$  and  $\mathbf{y}$ .

- 1: Compute a set of the previous requests  $\Phi_i$  for each request  $v_i$ :  $\Phi_0 \leftarrow \{v_0\}$  and  $\Phi_i \leftarrow \{v_j | e_j + q_{ji} \leq e_i, j \in \{I\}, \forall i \in \{I\}\}$ ;
- 2: Set the necessary conditions:  $U[i][c] \leftarrow -\infty, \forall c < 0$  or  $\forall \Phi_i \not\supset \{v_0\}$  and  $U[0][c] \leftarrow 0, \forall c \geq 0$ ;
- 3: Compute the subproblems  $U[i][c]$  according to Eq.(12), i.e.,  $U[i][c] \leftarrow \max_{j \in \Phi_i \setminus \{i\}} U[j][c_{ji}] + u_{ji}, \forall i \geq 1, c \geq 0, v_0 \in \Phi_i$ ;
- 4: Get  $\mathbf{l}$  and  $\mathbf{y}$  from  $\max_{i \in \{0, 1, \dots, I\}} U[i][C]$ .

Meanwhile, the inequality of the moving cost and the time, i.e., Eq. (2) and Eq. (3) guarantees the right usage of Eq. (12). Constrained by Eq. (2) and Eq. (3), the crowdsourcing user directly move among different regions and need not consider the optimal problem of the cost and the time.

According to Eq. (12), an optimal algorithm is proposed. **Algorithm 1** shows the concrete steps to indicate the response of the crowdsourcing users to the crowdsourcing requesters. That is, Step 1 computes the set of previous requests for every sorted request. Step 2 and 3 present the complete implementation process. More importantly, **Theorem 2** indicates that the proposed algorithm has the optimal system.

**Theorem 2:** **Algorithm 1** has the maximum system to solve the user recruitment problem with cost constraints with only one crowdsourcing user. Meanwhile, the computational complexity of the proposed algorithm is  $\mathcal{O}(I^2(C + p_{max}))$  in which  $p_{max}$  is the maximum item of matrix  $\mathbf{P}$ .

*Proof:* The user recruitment problem with cost constraints of only one crowdsourcing user has the best substructure. According to the utility  $U[i][c]$  and **Proposition 2**, it has  $|\Phi_i|$  that is the set of previous states for  $U[i][c]$ . The maximum value of  $U[i][c]$  depends on the optimal utility among the subproblems of  $|\Phi_i|$ . As a result, the solution to get the maximum value of  $U[i][c]$  is related to the solution to all the previous maximum problems, i.e.,  $|\Phi_i|$ . **Algorithm 1** utilizes the optimal value of each subproblem of  $U[i][c]$  to get the maximum value of  $U[i][c]$ . Thus, the proposed algorithm has the optimal system to the user recruitment problem with only one crowdsourcing user. Eq. (12) shows that  $U[i][c] (i \leq I, c \leq C)$  has disjoint sub-problems, whose number is no more than  $(I + 1) \times (C + p_{max} + 1)$  under the constraints of  $i$  and  $c$ . By comparing  $|\Phi_i| (\leq I)$  sub-problems, the optimal solution is derived. Thus, the computational complexity of the proposed algorithm is  $\mathcal{O}(I^2(C + p_{max}))$ . ■

## VI. OPTIMAL RECRUITMENT ALGORITHM WITH MULTIPLE CROWDSOURCING USERS

### A. Basic Idea of GPA

Here, we investigate the user recruitment problem with cost constraints in which there are several users to support the VSE service, i.e.,  $I \gg J \geq 1$ . Based on **Algorithm 1**, we propose a novel solution, i.e., graph-partition-based algorithm

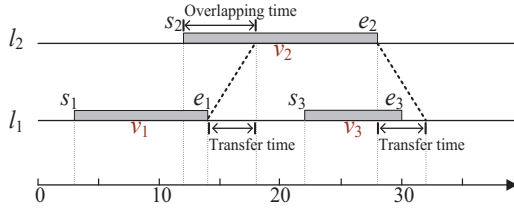


Fig. 6. An instance to compute  $\theta$  and  $\gamma$ .

(GPA). The solution idea of GPA is to *reduce the number of the regions that the crowdsourcing users move on the high-cost link*. Constrained by the total cost of the whole system  $C$ , the number of link transfers with low cost is increasing as a link transfer with high cost is removed. As a result, the crowdsourcing users can support the VSE services of more crowdsourcing requesters. According to the basic idea, we implement a graph-partition-based algorithm. That is, the requests from crowdsourcing requesters are clustered into a group of disjoint partitions, each of which is supported by a crowdsourcing user. In order to increase more link transfers, it needs some partition strategy to remove or decrease the links with high cost.

#### Graph-partition-based Algorithm Overview:

- **Step 1 (Requests Partition).** The requests are clustered into  $J$  different partitions by the popular normalized cut spectral clustering method. In the clustering process, we consider a tradeoff criterion between requests' overlapping degree and transfer cost.
- **Step 2 (Available Cost Allocation).** Crowdsourcing users are dispatched into those  $J$  partitions one by one based on their spatial distances and one user is responsible for one partition by **Algorithm 1**. Then the total available cost is allocated to different crowdsourcing users by some methods such as branch-and-bound or greedy approach.

#### B. Request Partition by Normalized Cut Spectral Clustering

In order to efficiently divide the requests, we propose a request partition algorithm based on the normalized cut spectral clustering technique. The core problem is how to cluster the similar requests into a partition. To this end, it needs some important metrics to reasonably compute the similarity among the requests. The first one is that any two requests in a partition are disjoint as much as possible. The second one is that the connectivity inside a partition should be low.

1) *Degree of Overlapping:* The degree of overlapping is used to evaluate the degree of coupling between a pair of two requests  $(v_i, v_j)$  satisfying  $e_i \leq e_j$ , which is computed as follows:

$$\theta(v_i, v_j) \triangleq 1 - \frac{(e_j - \max\{s_j, e_i + q_{ij}\})^+}{e_j - s_j}, \quad (13)$$

in which  $x^+ = \max\{x, 0\}$ .

2) *Degree of Connectivity:* The degree of connectivity is used to evaluate the relevancy between a pair of two requests  $(v_i, v_j)$  satisfying  $e_i \leq e_j$ , which is computed as follows:

$$\gamma(v_i, v_j) \triangleq \frac{p_{ij}}{p_{max}}. \quad (14)$$

Fig. 6 takes three requests (i.e.,  $v_1, v_2$  and  $v_3$ ) as an example to compute the degree of overlapping and the degree of connectivity. The time of the requests is  $[3, 14]$ ,  $[12, 28]$  and  $[22, 30]$ , respectively. The moving time from region  $l_1$  to  $l_2$  is 4 and the corresponding cost is  $p_{l_1, l_2} = p_{l_2, l_1} = 1$ . According to **Proposition 2**, when some crowdsourcing user offers the VSE service for request  $v_1$  and  $v_2$ , his path is from  $v_1$  to  $v_2$ . Therefore, the disjoint time of request  $v_1$  and  $v_2$  is  $e_2 - e_1 - p_{12} = 10$ , and  $\theta(v_1, v_2) = 1 - 10/(28 - 12) = 0.375$ . Besides,  $\theta(v_1, v_3) = 0$  and  $\theta(v_2, v_3) = 1$ . Due to  $p_{max} = 1$ ,  $\gamma(v_1, v_2) = 1$ ,  $\gamma(v_1, v_3) = 0$  and  $\gamma(v_2, v_3) = 1$ . It is obvious to find that the degree of overlapping and the degree of connectivity well reflect the coupling and the relevancy between any two requests.

3) *Degree of Similarity:* The degree of similarity of a pair of requests  $(v_i, v_j)$  is computed as  $\alpha_{ij} = \frac{1}{\theta + \beta\gamma}$ , in which  $\beta$  is a weight knob of the degree of overlapping and the degree of connectivity.

$\mathbf{W} = [\alpha_{ij}]$  is a matrix, in which each item  $\alpha_{ij}$  is the degree of the similarity of any two requests  $v_i$  and  $v_j$ .  $\mathbf{L}$  is a diagonal matrix, in which the  $i$ -th diagonal item is the sum of the items in the  $i$ -th row of  $\mathbf{W}$ .  $D_r$  is the  $r$ -th set of requests to be partitioned and  $D = \cup_{r=1}^J D_r$ .  $\mathbf{e}_r$  is a  $I \times 1$  indicator vector used to implement the  $r$ -th partition of requests, i.e.,  $\mathbf{e}_r \in \{0, 1\}^I$ . That is, there exists the nonzero elements in  $\mathbf{e}_r$  if the  $r$ -th partition has the new request. The objective is to find a reasonable division  $\mathbf{E} = (\mathbf{e}_1, \mathbf{e}_2, \dots, \mathbf{e}_J)$ , that combines the degree of overlapping and the degree of connectivity, i.e.,

$$\min_{\mathbf{E}} \sum_{r=1}^J \frac{\mathbf{e}_r^T (\mathbf{L} - \mathbf{W}) \mathbf{e}_r}{\mathbf{e}_r^T \mathbf{L} \mathbf{e}_r} = \sum_{r=1}^J \frac{\sum_{v_i \in D_r, v_j \notin D_r} \alpha_{ij}}{\sum_{v_i \in D_r, v_j \in D} \alpha_{ij}}. \quad (15)$$

In order to solve the above minimum problem, we propose a normalized spectral clustering algorithm. In brief, the basic idea of the algorithm is that the minimum problem is relaxed as an eigenvalue one, which is solved by an integer approach constrained by the binary condition.

4) *Solving the relaxed optimization of the minimum problem:* By introducing the idea of [42], the solution of Eq. (15) with the lower bound is

$$\min_{\mathbf{Y}^T \mathbf{Y} = \mathbf{I}} \text{tr} \mathbf{Y}^T (\mathbf{I} - \mathbf{L}^{-1/2} \mathbf{W} \mathbf{L}^{-1/2}) \mathbf{Y} = \sum_{j=1}^J \lambda_j, \mathbf{Y} \in R^{I \times J} \quad (16)$$

in which  $\lambda_j$  is the  $j$ -th smallest eigenvalue of  $\mathbf{I} - \mathbf{L}^{-1/2} \mathbf{W} \mathbf{L}^{-1/2}$ . We use matrix  $\mathbf{U}$  to obtain the lower bound of Eq. (15) by setting  $\mathbf{Y} = \mathbf{U}$ . That is, the column in matrix  $\mathbf{U}$  is the eigenvector referring to the  $J$  eigenvalues of  $\mathbf{I} - \mathbf{L}^{-1/2} \mathbf{W} \mathbf{L}^{-1/2}$ . Therefore, the relaxed solution of Eq. (15) is computed by  $\hat{\mathbf{E}} = \mathbf{L}^{-1/2} \mathbf{U}$ .

5) *Obtaining binary solution of the relaxation problem:* Suppose that  $\hat{\mathbf{E}}$  offers an approximate solution of  $\mathbf{E}$  and has the non-integer elements. Thus, it is necessary to change  $\hat{\mathbf{E}}$ 's element as a binary one. We use the  $k$ -means approach to solve the above problem. At first, each row of  $\hat{\mathbf{E}}$  is normalized to norm 1, i.e.,  $e_{ij} \leftarrow e_{ij} / (\sum_{m=1}^J e_{im})^{1/2}$ . Then, we utilized a  $k$ -means approach to cluster the rows into  $J$  partitions. Meanwhile, the memory and the time of spectral clustering to solve the large-scale data sets are huge. Therefore, parallelism



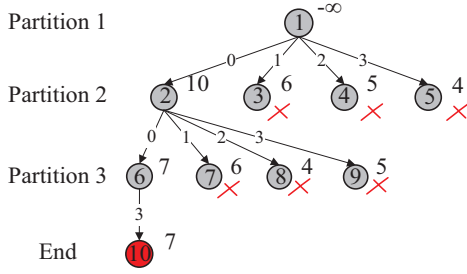


Fig. 7. An example to show the branch-and-bound process.

realization [43] can efficiently speed up spectral clustering algorithm on very large-scale datasets.

### C. Branch-and-Bound/Greedy Cost Allocation

By using the normalized cut spectral clustering algorithm, the requests of all the crowdsourcing requesters are clustered as  $J$  groups, which is defined as  $\{D_r^* | r = 1, \dots, J\}$ . Crowdsourcing users compute the average Euclidean distance between his location and each request in any group. According to the results, crowdsourcing users select the nearest group and offer the VSE service. We use **Algorithm 1** to obtain the optimal solution for every request group.  $U_r[c]$  ( $0 \leq c \leq C$ ) is defined as optimal utility of the whole system under the condition of the total cost of  $c$  of the  $r$ -th request group  $D_r^*$ . On the other hand, if the total cost is not allocated to the partitions in advance, it is hard to get the optimal utility of the whole system due to the limited cost. Therefore, it is necessary to make the reasonable allocation of the cost for the request group. To this end, the  $r$ -th request group is allocated by the cost  $c_r$ . As a result, the optimal problem to maximize the utility of the whole system is

$$\begin{aligned} \max \quad & \sum_r U_r[c_r] \\ \text{s. t.} \quad & \sum_r c_r \leq C. \end{aligned} \quad (17)$$

In essence, the maximization problem is combinatorial optimization. In **Algorithm 1**, the maximization utility of each round is monotonously increasing as the cost  $c$  is increasing. According to the monotonicity of the utility with the given cost, an optimal branch-and-bound search algorithm is proposed to reasonably allocate the cost to the request groups.

1) *Branch-and-bound cost allocation*: Suppose that the system allocates the cost  $\{c_1, c_2, \dots, c_J\}$  to request groups sequentially. Thus, an important proposition is derived as follows:

**Proposition 3**: Assume that the cost  $h_k$  is allocated to the  $k$ -th request partition, the corresponding utility of the system is  $g_k$ . For the rest request partitions, the total utility of the system is no more than

$$u_k = g_k + \sum_{r=k+1}^J U_r[C - h_k]. \quad (18)$$

*Proof*: Since the utility  $U_r[c]$  is a monotone increasing function and the rest request partitions are allocated the

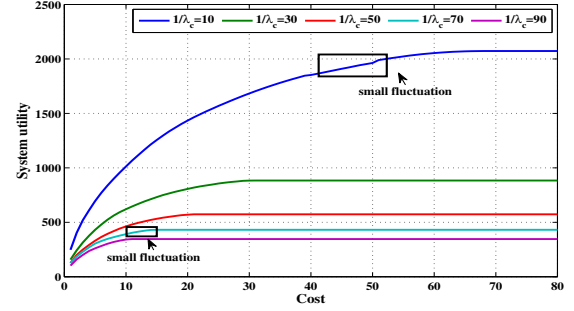


Fig. 8. An example to show approximate increasing concave property of  $U_r$ .

remaining cost to. Thus, the rest request partitions get the maximum utility, which is determined by  $u_k$ . ■

According to **Proposition 3**, we use the depth-first search approach to implement the allocation of the remaining cost to the request partitions, in which the upper bound of the allocated cost is first selected. That is, when a new leaf node is inserted to a search tree, the nodes with smaller values are removed. Finally, there is only one leaf node that is the optimal solution to the cost allocation.

Fig. 7 shows an example to present the detailed process of the branch-and-bound, in which  $C = 3$ ,  $U_1 = (1, 1, 2, 3)$ ,  $U_2 = (1, 2, 2, 4)$ , and  $U_3 = (0, 1, 3, 5)$ . Every node is labelled by a value that represents the upper bound of the problem derived by Eq. (18), while every edge is labelled by a value that refers to the cost allocated on the corresponding partition. For example, when  $U_1$  is allocated 0 cost, the upper bound of the total utility on node 2 is  $U_1[0] + U_2[3] + U_3[3] = 1 + 4 + 5 = 10$ , when  $U_1$  is allocated 1, 2 and 3 cost, the upper bounds of total utility on node 3, 4, 5 are 6, 5, 4 respectively. Since the left node in the second layer of the tree has the maximum value of 10, we continue to only analyze its sub-nodes and repeat the process. Meanwhile, the other nodes in the tree are removed. Thus, the optimal utility in the example is 7 under the solution  $\{0, 0, 3\}$ .

2) *Greedy cost allocation*: On one hand, the branch-and-bound search approach implements the reasonable cost allocation and guarantees the optimal utility of the whole system. On the other hand, the computational complexity of the approach is relatively high, especially when the total cost  $C$  is large enough. In order to decrease the computational complexity, we propose a greedy approach.

- **Step 1.** Set the maximum cost length  $c_0$ , a middle vector to allocate the cost  $\mathbf{c}' = \{c'_1, c'_2, \dots, c'_J\}$ .
- **Step 2.** Compute a novel metric of  $U_r$  in  $[c'_i, c'_i + c_0]$  to evaluate the efficiency of the cost increment.
- **Step 3.** Solve the corresponding cost increment

$$(r^*, c_s^*) = \arg \max \left\{ \frac{U_r[c'_i + c_s] - U_r[c'_i]}{c_s} \mid \forall r, c_s \leq c_0 \right\}. \quad (19)$$

- **Step 4.** Update  $c'_{r^*} = c'_{r^*} + c_s^*$ .
- **Step 5.** Repeat Step 2 4 until the cost is beyond the total available cost.

In order to guarantee the efficiency of the proposed greedy approach,  $U_r[c_r]$  is approximately regarded as an increasing concave function. Fig. 8 shows an instance to present the function  $U_r[c_r]$  with little fluctuation. When  $U_r[c_r]$  is an increasing concave function, by analyzing the KKT (Karush–Kuhn–Tucker) condition, i.e.,  $\frac{\partial U_m}{\partial c_m} = \frac{\partial U_n}{\partial c_n}$ , the cost allocation to maximize the utility of the system is computed at the equal derivative point. As a result, the proposed greedy approach can obtain the optimal solution in the example. Meanwhile, the small fluctuation possibly has a bad influence on the optimal solution. To this end, the cost length  $c_0$  should be greater than 1 to eliminate negative effect brought by the small fluctuation and get the better utility.

## VII. FURTHER DISCUSSION

In this section, we discuss the least expected budget  $C_0$  to achieve the maximum utility. The discussion would help central controller decide capital investment on the system. Actually, on the one hand, some requests may be denied and discarded because of limited budget; on the other hand, investing too much money is unnecessary as there exist upper bound of utility for a given system.

To simplify the discussion and highlight the key insights, we introduce an ideal model.

**Ideal Model:** In the  $k$ -th region, the requests come following a poisson process where interarrival times are independent with each other and obey the exponential distribution with parameter  $\lambda_k$ . The utility is *one-time bonus* i.e., the system gains the request's utility once one crowdsourcing user arrives at this request. Moreover, the transfer time among any two regions is assumed to be 0 and the moving cost among any two regions is constant, denoted as  $p$ .

Based on this ideal model, we analyse the least expected budget to achieve the maximum system utility for both single and multiple crowdsourcing user case.

**Proposition 4:** Based on the ideal model, the least expected budget  $C_0^s$  to achieve the maximum utility for single crowdsourcing user case is  $C_0^s = \frac{pT((\sum_{k=1}^K \lambda_k)^2 - \sum_{k=1}^K \lambda_k^2)}{\sum_{k=1}^K \lambda_k}$ .

*Proof:* First, we consider any two regions  $k_i$  and  $k_j$  and the transfer number  $X_{ij}$  from  $k_i$  to  $k_j$ . During one interarrival time  $[t_1, t_2]$  in region  $k_i$ , the probability that there exist some requests in region  $k_j$  is  $1 - e^{-\lambda_j(t_2 - t_1)}$ . Therefore, the expected transfer number  $E(X_{ij})$  from region  $k_i$  to region  $k_j$  in one interarrival time is,

$$E(X_{ij}) = \int_0^{+\infty} (1 - e^{-\lambda_j t}) \lambda_i e^{-\lambda_i t} dt = \frac{\lambda_j}{\lambda_i + \lambda_j} \quad (20)$$

As the expected interarrival time in region  $k_i$  is  $\frac{1}{\lambda_i}$ , therefore, the expected total transfer number from  $k_i$  to  $k_j$  is  $E(X_{ij}) \times \frac{T}{1/\lambda_i} = \frac{T\lambda_i\lambda_j}{\lambda_i + \lambda_j}$ . Considering that the regions  $k_{-i} = \Lambda - \{k_i\}$ , since independent poisson processes have the *super-positioning* property, therefore, the requests in  $k_{-i}$  is also poisson and have a rate of  $\lambda_{-i} = \sum_{k_m \in k_{-i}} \lambda_m$ . Then, based on the above analysis, the expected total transfer number in the system is,

$$E(X) = \sum_{i=1}^K E(X_{i,-i}) = \frac{T \sum_i \lambda_i \lambda_{-i}}{\sum_i \lambda_i}. \quad (21)$$

As such, the least expected budget is  $pE(X) = \frac{pT((\sum_{k=1}^K \lambda_k)^2 - \sum_{k=1}^K \lambda_k^2)}{\sum_{k=1}^K \lambda_k}$ . ■

Next, we analyse the multiple crowdsourcing users case. Based on the ideal model, estimating the total available cost  $C_0^m$  to achieve the maximum system utility is equivalent to dividing these  $K$  regions into  $J$  good partitions  $\mathcal{P}$ , i.e.,  $C_0^m = \min_{\mathcal{P}} \sum_{i=1}^J C_0(\mathcal{P}_i) = \min_{\mathcal{P}} \{pT\lambda_c - pT \sum_{i=1}^J \frac{\sum_{k_j \in \mathcal{P}_i} \lambda_j^2}{\sum_{k_j \in \mathcal{P}_i} \lambda_j}\}$ , where  $\lambda_c = \sum_{k=1}^K \lambda_k$ .

**Proposition 5:** Based on the ideal model, the least expected budget  $C_0^m$  to achieve the maximum utility for multiple crowdsourcing users case is no more than  $(1 - \frac{1}{K})pT\lambda_c$ , i.e.,  $C_0^m \leq (1 - \frac{1}{K})pT\lambda_c$ .

*Proof:* From Cauchy-Schwarz inequality, we have,

$$\frac{\sum_{k_j \in \mathcal{P}_i} \lambda_j^2}{\sum_{k_j \in \mathcal{P}_i} \lambda_j} \geq \frac{\sum_{k_j \in \mathcal{P}_i} \lambda_j}{|\mathcal{P}_i|} \quad (22)$$

Moreover, the following inequality holds:

$$\sum_{i=1}^J \frac{\sum_{k_j \in \mathcal{P}_i} \lambda_j}{|\mathcal{P}_i|} \geq \frac{\sum_i \sum_{k_j \in \mathcal{P}_i} \lambda_j}{\sum_i |\mathcal{P}_i|} = \frac{\lambda_c}{K} \quad (23)$$

Therefore,  $C_0^m \leq pT\lambda_c - pT \sum_i \frac{\sum_{k_j \in \mathcal{P}_i} \lambda_j^2}{\sum_{k_j \in \mathcal{P}_i} \lambda_j} \leq pT\lambda_c - \frac{pT\lambda_c}{K}$ .

Hence, we have this proposition. ■

Specially, when  $\lambda_i = \lambda_j = \lambda$ , the result is reduced to be  $C_0^m = pT\lambda_c - pTJ\lambda$ . That is, if  $J \leq K$ , the least expected total budget  $C_0^m$  can linearly decrease with the increase of crowdsourcing users' number.

## VIII. PERFORMANCE EVALUATION

### A. Simulation Setup

1) *Parameter Setting:* In the experiments, the area consists of  $50 \times 45$  sub-regions, each of which is a square and the corresponding side length is 5 meters. We adopt the following two models to show the trajectory of mobile users:

- **Random Waypoint Model (RWM) [44].** The distribution of mobile users is relatively uniform.
- **Campus Waypoint Model (CWM) [45].** The distribution of mobile users is not uniform.

The time that each crowdsourcing user spends in a region is derived from the Pareto distribution [46], in which the scale and shape parameters are 2 and 5, respectively. The time that the crowdsourcing requesters spend in the video-related applications is derived from the gamma distribution [47], in which in which the scale and shape parameters are 2 and 4, respectively. The number of crowdsourcing requests that every region receives is derived from the Poisson process and  $\lambda_c \in [0.01, 0.1]$ .

2) *Comparison Algorithms:* We compare the proposed algorithm with multiple benchmark ones. The algorithmic descriptions are just listed as follows:

- **Region Division (RD) and Branch-and-Bound/Greedy Cost Allocation:** In order to evaluate the influence of different request partitions, we realize a region-division method. In this method, the whole area is first divided into  $J$  parts given their spatial correlations, then all requests

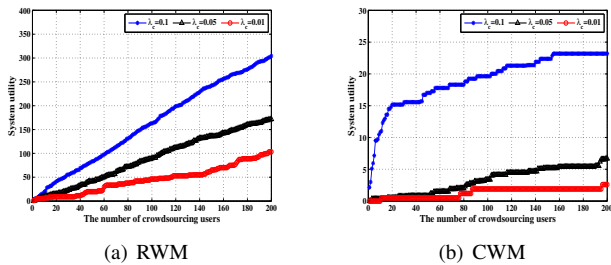


Fig. 9. The impact of the number of crowdsourcing users on the utility of the whole system with no path guidance.

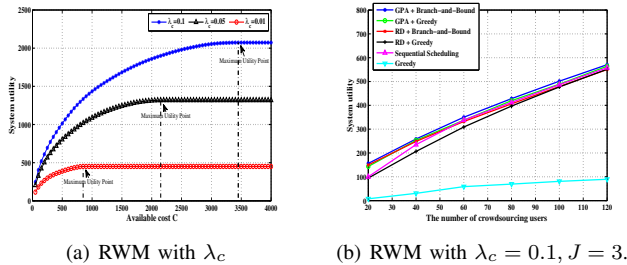


Fig. 10. The impact of the budget cost on the utility of the whole system.

are simply classified into different groups according to their own locations. Similar with GPA, the optimal routing scheduling algorithm is adopted to address each group of requests and the branch-and-bound/greedy algorithm is used to allocate the total available cost.

- *Sequential Scheduling*: The total available cost is equally allocated to different  $J$  crowdsourcing users. Then we randomly pick out one crowdsourcing user and make a scheduling decision by the optimal routing scheduling algorithm. We update the requests status by removing the requests being served. This process is repeated until all crowdsourcing users have been scheduled.
- *Greedy Scheduling*: This algorithm proceeds as a best-effort style. That is, for each request, we calculate the corresponding utility-cost ratio (i.e., utility increment divided by cost increment) of different crowdsourcing users and allocate this request to the crowdsourcing user with the maximum ratio. Of course, the request would be discarded if there is no utility increment i.e., the maximum ratio is 0. It repeats the above steps and stop if the cost exceeds the remaining one.

3) *Environmental Setting*: The algorithms are implemented under the MATLAB environment on a machine with two Intel Core i5-4278U 2.60GHz processors and 8GB RAM.

## B. Movement Control Influence Evaluation

We evaluate the influence of the number of crowdsourcing users and the arrival rates of crowdsourcing requests on the utility of the whole system without any movement control. Fig. 9 shows that the number of crowdsourcing users and the arrival rates of crowdsourcing requests have the significant influence on the utility. That is, as the number of crowdsourcing users is increasing, the utility of the whole system in both RWM

and CWM is increasing. The difference is that the curve in RWM is smoother than that in CWM. Different from RWM, the distribution of CWM is not uniform, implying that there are some gathering points of crowdsourcing users and some places with few of users in campus. In particular, the utility of the system is slow increasing when the crowdsourcing users of the gathering points in CWM offer the VSE service. If some requests do not receive the VSE service from crowdsourcing services, the utility of the system is low.

We evaluate the influence of the budget cost on the utility of the system. Fig. 10(a) shows a special case, in which there is only one crowdsourcing user. It is obvious to find that as the cost is increasing, the utility of the system is increasing. The curve in Fig. 10(a) is an approximate increasing concave function. Whatever parameter  $\lambda_c$  is, there exists the upper bound of the utility of the system even if the total cost is large enough. Thus, it is important to set the reasonable available cost of the whole system.

## C. Comparisons among Benchmark Algorithms

1) *Impact of the number of crowdsourcing users*: We evaluate the impact of the number of crowdsourcing users on different performance metrics, including the utility, the time, and the cost allocation fairness. Fig. 11(a) shows that as the number of crowdsourcing users is increasing, the utility of the system in all the benchmark algorithms is increasing. The finding implies that with the addition of more crowdsourcing users, the distance of crowdsourcing users to their customers is closer. That is, the moving cost of crowdsourcing users is decreasing as the number of crowdsourcing users is increasing. Meanwhile, the increment speed of the utility of the whole system is decreasing, implying that the increase of  $J$  makes the requests better finished.

On the other hand, Fig. 11(a) shows that clustering the crowdsourcing requests improves the utility of the whole system. Meanwhile, Fig. 11(b) shows that clustering the crowdsourcing requests takes more time. It is important to consider the tradeoff between the utility of the system and the time consumption by analyzing the overlapping degree of the crowdsourcing requests and the cost of moving the region. Fig. 10(a) also shows that the greedy cost allocation approach could obtain the approximate optimal utility and has little gap to the optimal algorithms. More importantly, the time consumption of the greedy cost allocation approach is very low. Therefore, the approach is well suited to the larger cost. We also evaluate the impact of the number of crowdsourcing users on the cost allocation fairness. We use the mean absolute deviation (MAD) to measure the cost allocation fairness. The greater the value of the mean absolute deviation, the worse the cost allocation fairness is. Fig. 11(c) shows that all the approaches have a similar cost allocation fairness.

2) *Impact of the total cost  $C$* : We evaluate the impact of the total cost on the utility of the system. Fig. 10(b) shows that as the total cost is increasing, the utility of the system of all the approaches is increasing. The utility of the greedy approach is the worst compared to the other approaches.

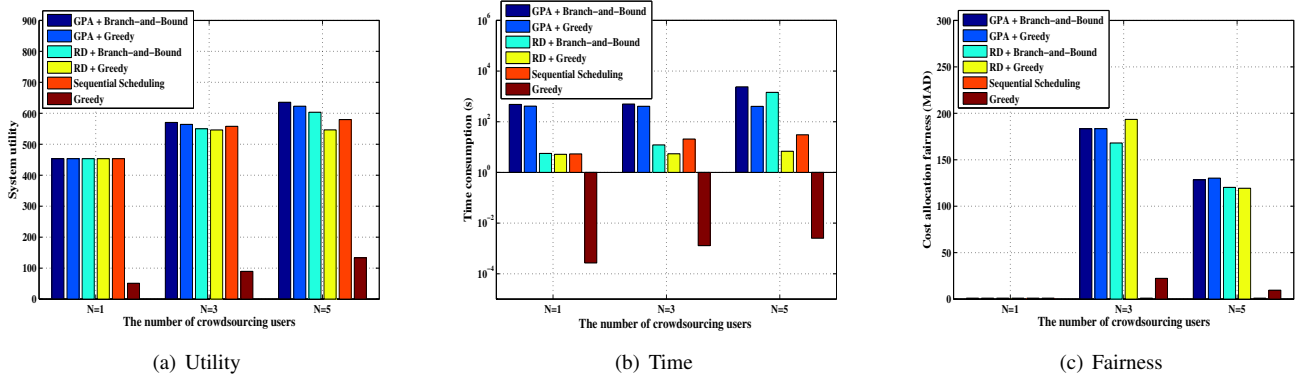
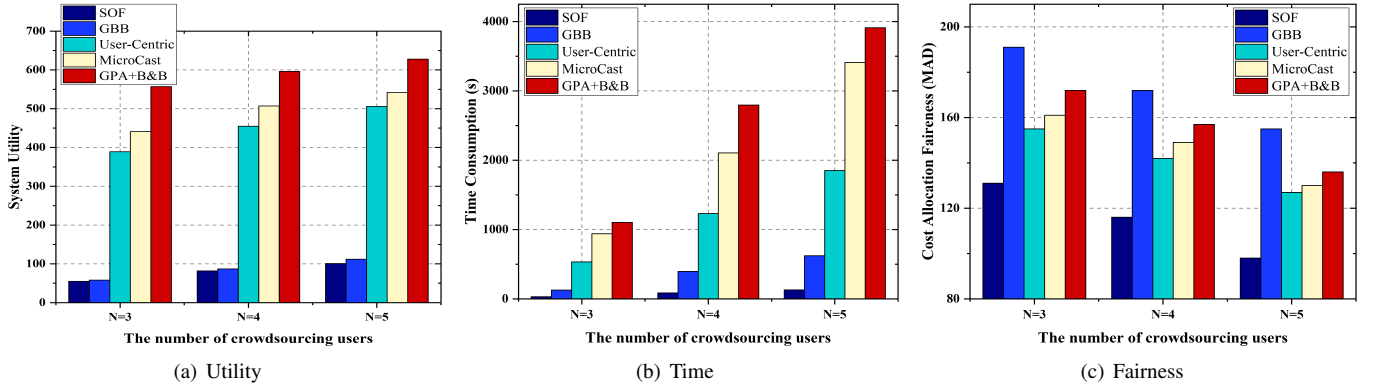
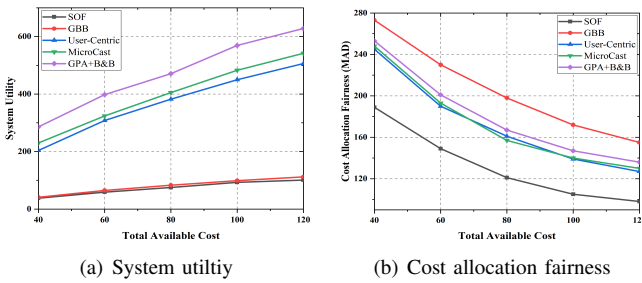

 Fig. 11. The impact of the number of crowdsourcing users  $J$  on different performance metrics among the benchmark algorithms with  $\lambda_c = 0.1, C = 120$ .

 Fig. 12. The impact of the number of crowdsourcing users  $J$  on different performance metrics among the typical algorithms with  $\lambda_c = 0.1, C = 120$ .


Fig. 13. The influence of available cost on system utility and cost allocation fairness for the typical algorithms.

#### D. Comparison with Typical algorithms

In the above analysis, GPA with Branch-and-Bound (abbrv. GPA+B&B) has the better system utility than that of the other methods. In addition, we also compare GPA+B&B with the typical algorithms about network cooperation with D2D communication, including SOF [48], GBB [48], User-Centric [30], and MicroCast [31]. However, those algorithms can not be directly compared with GPA+B&B, since they are not fully suited to the setting of the paper. To this end, we properly update these algorithms to better compare them in terms of system utility, time consumption, and cost allocation fairness.

1) *Comparison with typical algorithms*: Fig. 12 shows the results of the typical algorithms in multiple evaluation criteria. Fig. 12(a) indicates that GPA+B&B has the absolute advantage

in the system utility, whatever the number of crowdsourcing users is. On the other hand, Fig. 12(b) and Fig. 12(c) show that the corresponding cost of GPA+B&B in time and fairness is relatively higher, compared to the others. Therefore, it is necessary to improve GPA+B&B to decrease the time consumption and fairness, which is our future research direction.

2) *Effect of total available cost  $C$* : Fig. 13 shows the effect of total available cost on our proposed algorithm and the typical ones. The results indicate that the total available cost has the important effect on the algorithms in terms of system utility and cost allocation fairness. That is, Fig. 13(a) shows that as the total available cost is increasing, the system utility of all the algorithms is increasing. In particular, the total available cost has the higher effect on GPA+B&B, MicroCast, and User-Centric. Fig. 13(b) shows that as the total available cost is increasing, the cost allocation fairness of all the algorithms is decreasing. It implies that the increase of the total available cost brings the increase of the fairness.

## IX. CONCLUSION

In this paper, we focus on how to utilize the key component in a digital-twin-enabled 6G network, i.e., cybertwin, to decrease the network delay of mobile devices and enhance the quality of video streaming-related services with the higher traffic demands. We leverage the cybertwin as a centric controller and adopt the crowdsourcing paradigm and D2D communication technology to attract a lot of mobile



users to follow the specified path and share their network resources. We formulate the path plan as a problem of user recruitment optimization with cost constraints. We design the optimal solution in two different cases, including only one crowdsourcing user and multiple users. Experimental results show the proposed algorithms facilitate the quality of high-quality video enhancement service.

Although the paper presents an efficient application of digital-twin-enabled 6G mobile network for mobile video streaming with high quality, it is worthwhile to analyze the possible improvements as the future research work. In the crowdsourcing scenario, the central controller that receives sensitive information from mobile users should be trusted. It needs to investigate the potential privacy leakage risk, i.e., potential users' location information leaked to the adversary, and the corresponding protection measures. In addition, it is necessary to study the balance between cost and fairness, as the user with the high cost cannot be selected for a long time, thereby having the low fairness.

#### ACKNOWLEDGMENT

Our thanks to the reviewers for their constructive comments and suggestions to improve the quality of the manuscript. This work was supported in part by the National Natural Science Foundation of China under Grant no. 92267104.

#### REFERENCES

- [1] F. Tang, Y. Kawamoto, N. Kato, and J. Liu, "Future intelligent and secure vehicular network toward 6g: Machine-learning approaches," *Proc. IEEE*, vol. 108, no. 2, pp. 292–307, 2020.
- [2] K. Sheth, K. Patel, H. Shah, S. Tanwar, R. Gupta, and N. Kumar, "A taxonomy of AI techniques for 6g communication networks," *Comput. Commun.*, vol. 161, pp. 279–303, 2020.
- [3] H. Xu, J. Wu, J. Li, and X. Lin, "Deep-reinforcement-learning-based cybertwin architecture for 6g iiot: An integrated design of control, communication, and computing," *IEEE Internet Things J.*, vol. 8, no. 22, pp. 16 337–16 348, 2021.
- [4] Y. Lu, X. Huang, K. Zhang, S. Maharjan, and Y. Zhang, "Low-latency federated learning and blockchain for edge association in digital twin empowered 6g networks," *IEEE Trans. Ind. Informatics*, vol. 17, no. 7, pp. 5098–5107, 2021.
- [5] A. Hazra, M. Adhikari, T. Amgoth, and S. N. Srirama, "Stackelberg game for service deployment of iot-enabled applications in 6g-aware fog networks," *IEEE Internet Things J.*, vol. 8, no. 7, pp. 5185–5193, 2021.
- [6] Q. Yu, J. Ren, Y. Fu, Y. Li, and W. Zhang, "Cybertwin: An origin of next generation network architecture," *IEEE Wireless Communications*, vol. 26, no. 6, pp. 111–117, 2019.
- [7] I. Sandvine, "Global internet phenomena report," *North America and Latin America*, 2016.
- [8] R. Anderson, D. Gallup, J. T. Barron, J. Kontkanen, N. Snavely, C. Hernández, S. Agarwal, and S. M. Seitz, "Jump: virtual reality video," *ACM Transactions on Graphics (TOG)*, vol. 35, no. 6, pp. 1–13, 2016.
- [9] M. Yamaguchi, S. Mori, P. Mohr, M. Tatzgern, A. Stanescu, H. Saito, and D. Kalkofen, "Video-annotated augmented reality assembly tutorials," in *Proceedings of the 33rd Annual ACM Symposium on User Interface Software and Technology*, 2020, pp. 1010–1022.
- [10] G. K. Illahi, T. V. Gemert, M. Siekkinen, E. Masala, A. Oulasvirta, and A. Ylä-Jääski, "Cloud gaming with foveated video encoding," *ACM Trans. Multim. Comput. Commun. Appl.*, vol. 16, no. 1, pp. 7:1–7:24, 2020.
- [11] A. De Vita, R. Garello, V. Mignone, A. Morello, and G. Taricco, "Mobile and broadcast networks cooperation for high quality mobile video: a win-win approach," 2016.
- [12] C. Chakraborty and J. J. P. C. Rodrigues, "A comprehensive review on device-to-device communication paradigm: Trends, challenges and applications," *Wirel. Pers. Commun.*, vol. 114, no. 1, pp. 185–207, 2020.
- [13] A. Asadi, V. Mancuso, and R. Gupta, "DORE: an experimental framework to enable outband D2D relay in cellular networks," *IEEE/ACM Trans. Netw.*, vol. 25, no. 5, pp. 2930–2943, 2017.
- [14] L. Wang, Z. Yu, D. Yang, T. Ku, B. Guo, and H. Ma, "Collaborative mobile crowdsensing in opportunistic d2d networks: A graph-based approach," *ACM Transactions on Sensor Networks (TOSN)*, vol. 15, no. 3, pp. 1–30, 2019.
- [15] A. Ortiz, A. Asadi, M. Engelhardt, A. Klein, and M. Hollick, "Cbmos: Combinatorial bandit learning for mode selection and resource allocation in d2d systems," *IEEE Journal on Selected Areas in Communications*, vol. 37, no. 10, pp. 2225–2238, 2019.
- [16] Y. Yan, B. Zhang, and C. Li, "Network coding aided collaborative real-time scalable video transmission in D2D communications," *IEEE Trans. Veh. Technol.*, vol. 67, no. 7, pp. 6203–6217, 2018.
- [17] D. Wu, Q. Liu, H. Wang, Q. Yang, and R. Wang, "Cache less for more: Exploiting cooperative video caching and delivery in d2d communications," *IEEE Transactions on Multimedia*, vol. 21, no. 7, pp. 1788–1798, 2018.
- [18] J. Lin, M. Li, D. Yang, and G. Xue, "Sybil-proof online incentive mechanisms for crowdsensing," in *IEEE Conference on Computer Communications (INFOCOM)*, 2018, pp. 2438–2446.
- [19] M. Karaliopoulos, I. Koutsopoulos, and L. Spiliopoulos, "Optimal user choice engineering in mobile crowdsensing with bounded rational users," in *IEEE Conference on Computer Communications (INFOCOM)*, 2019, pp. 1054–1062.
- [20] W. Zhi, K. Zhu, Y. Zhang, and L. Zhang, "Hierarchically social-aware incentivized caching for D2D communications," in *IEEE International Conference on Parallel and Distributed Systems, ICPADS*, 2016, pp. 316–323.
- [21] X. Xu, Q. Cai, G. Zhang, J. Zhang, W. Tian, X. Zhang, and A. X. Liu, "An incentive mechanism for crowdsourcing markets with social welfare maximization in cloud-edge computing," *Concurr. Comput. Pract. Exp.*, vol. 33, no. 7, p. 1, 2021.
- [22] A. H. Sodhro, S. Pirbhulal, Z. Luo, K. Muhammad, and N. Zahid, "Toward 6g architecture for energy-efficient communication in iot-enabled smart automation systems," *IEEE Internet Things J.*, vol. 8, no. 7, pp. 5141–5148, 2021.
- [23] X. Zhang, J. Wang, and H. V. Poor, "Statistical delay and error-rate bounded qos provisioning for murrll over 6g CF M-MIMO mobile networks in the finite blocklength regime," *IEEE J. Sel. Areas Commun.*, vol. 39, no. 3, pp. 652–667, 2021.
- [24] —, "Statistical delay and error-rate bounded qos provisioning over mmwave cell-free M-MIMO and FBC-HARQ-IR based 6g wireless networks," *IEEE J. Sel. Areas Commun.*, vol. 38, no. 8, pp. 1661–1677, 2020.
- [25] D. Bhat, A. Rizk, M. Zink, and R. Steinmetz, "SABR: network-assisted content distribution for qoe-driven ABR video streaming," *ACM Trans. Multim. Comput. Commun. Appl.*, vol. 14, no. 2s, pp. 32:1–32:25, 2018.
- [26] P. Krishnan, K. Jain, P. G. Jose, K. Achuthan, and R. Buyya, "SDN enabled qoe and security framework for multimedia applications in 5g networks," *ACM Trans. Multim. Comput. Commun. Appl.*, vol. 17, no. 2, pp. 39:1–39:29, 2021.
- [27] H. Liang, H. Li, and W. Zhang, "A combinatorial auction resource trading mechanism for cybertwin based 6g network," *IEEE Internet of Things Journal*, 2021.
- [28] T. K. Rodrigues, J. Liu, and N. Kato, "Application of cybertwin for offloading in mobile multi-access edge computing for 6g networks," *IEEE Internet of Things Journal*, 2021.
- [29] Y.-D. Lin and Y.-C. Hsu, "Multihop cellular: A new architecture for wireless communications," in *IEEE Conference on Computer Communications (INFOCOM)*, vol. 3, 2000, pp. 1273–1282.
- [30] B. Chen, C. Yang, and A. F. Molisch, "Cache-enabled device-to-device communications: Offloading gain and energy cost," *IEEE Transactions on Wireless Communications*, vol. 16, no. 7, pp. 4519–4536, 2017.
- [31] A. Le, L. Keller, H. Seferoglu, B. Cici, C. Fragouli, and A. Markopoulou, "Microcast: Cooperative video streaming using cellular and local connections," *IEEE/ACM Transactions on Networking*, vol. 24, no. 5, pp. 2983–2999, 2015.
- [32] Y. Cao, T. Jiang, X. Chen, and J. Zhang, "Social-aware video multicast based on device-to-device communications," *IEEE Trans. Mob. Comput.*, vol. 15, no. 6, pp. 1528–1539, 2016.
- [33] Z. Liu, H. Song, and D. Pan, "Distributed video content caching policy with deep learning approaches for D2D communication," *IEEE Trans. Veh. Technol.*, vol. 69, no. 12, pp. 15 644–15 655, 2020.
- [34] N. Golrezaei, A. F. Molisch, A. G. Dimakis, and G. Caire, "Femto-caching and device-to-device collaboration: A new architecture for

wireless video distribution,” *IEEE Communications Magazine*, vol. 51, no. 4, pp. 142–149, 2013.

- [35] Z. Zhang, T. Zeng, X. Yu, and S. Sun, “Social-aware D2D pairing for cooperative video transmission using matching theory,” *Mobile Networks and Applications*, vol. 23, no. 3, pp. 639–649, 2018.
- [36] Y. Yan, B. Zhang, and C. Li, “Network coding aided collaborative real-time scalable video transmission in d2d communications,” *IEEE Transactions on Vehicular Technology*, vol. 67, no. 7, pp. 6203–6217, 2018.
- [37] D. Wu, Q. Liu, H. Wang, Q. Yang, and R. Wang, “Cache less for more: Exploiting cooperative video caching and delivery in D2D communications,” *IEEE Trans. Multim.*, vol. 21, no. 7, pp. 1788–1798, 2019.
- [38] F. Chen, C. Zhang, F. Wang, J. Liu, X. Wang, and Y. Liu, “Cloud-assisted live streaming for crowdsourced multimedia content,” *IEEE Transactions on Multimedia*, vol. 17, no. 9, pp. 1471–1483, 2015.
- [39] Y. Zhou, L. Chen, M. Jing, Z. Ming, and Y. Xu, “Performance analysis of thunder crystal: A crowdsourcing-based video distribution platform,” *IEEE Transactions on Circuits and Systems for Video Technology*, vol. 28, no. 4, pp. 997–1008, 2016.
- [40] J. Van Der Hooft, S. Petrangeli, T. Wauters, R. Huyssegems, P. R. Alfaca, T. Bostoen, and F. De Turck, “Http/2-based adaptive streaming of hevc video over 4g/lte networks,” *IEEE Communications Letters*, vol. 20, no. 11, pp. 2177–2180, 2016.
- [41] M. Zhanikeev, “Virtual wireless user: A practical design for parallel multiconnect using wifi direct in group communication,” in *International Conference on Mobile and Ubiquitous Systems: Computing, Networking, and Services*, 2013, pp. 782–793.
- [42] F. Bach and M. Jordan, “Learning spectral clustering,” *Advances in neural information processing systems*, vol. 16, no. 2, pp. 305–312, 2004.
- [43] W. Chen, Y. Song, H. Bai, C. Lin, and E. Y. Chang, “Parallel spectral clustering in distributed systems,” *IEEE Trans. Pattern Anal. Mach. Intell.*, vol. 33, no. 3, pp. 568–586, 2011.
- [44] J. Broch, D. A. Maltz, D. B. Johnson, Y.-C. Hu, and J. Jetcheva, “A performance comparison of multi-hop wireless ad hoc network routing protocols,” in *Proceedings of the 4th annual ACM/IEEE international conference on Mobile computing and networking*, 1998, pp. 85–97.
- [45] M. McNett and G. M. Voelker, “Access and mobility of wireless pda users,” *ACM SIGMOBILE Mobile Computing and Communications Review*, vol. 9, no. 2, pp. 40–55, 2005.
- [46] Z. Lu, X. Sun, and T. La Porta, “Cooperative data offloading in opportunistic mobile networks,” in *IEEE International Conference on Computer Communications (INFOCOM)*, 2016, pp. 1–9.
- [47] Y. Zhou, L. Chen, C. Yang, and D. M. Chiu, “Video popularity dynamics and its implication for replication,” *IEEE transactions on multimedia*, vol. 17, no. 8, pp. 1273–1285, 2015.
- [48] Y. Li and W. Wang, “Message dissemination in intermittently connected d2d communication networks,” *IEEE Transactions on Wireless Communications*, vol. 13, no. 7, pp. 3978–3990, 2014.



**Lianyong Qi** received his PhD degree in Department of Computer Science and Technology from Nanjing University, China. Now, he is a Professor of College of Computer Science and Technology, China University of Petroleum (East China), China. His research interests include recommender systems and services computing.



been selected as the Highly Cited Researcher of Clarivate 2021 and 2022. His research interests include edge intelligence and service computing.

**Xiaolong Xu** received the Ph.D. degree in computer science and technology from Nanjing University, China, in 2016. He is currently a Professor with the School of Software, Nanjing University of Information Science and Technology. He received the Best Paper Awards from the IEEE CBD 2016, IEEE CyberTech2021, IEEE iThings2022 and IEEE ISPA 2022, and the Outstanding Paper Award from IEEE SmartCity2021. He received the Outstanding Leadership Award of IEEE UIC 2022. He also received the Best Paper Award from Elsevier JNCA. He has



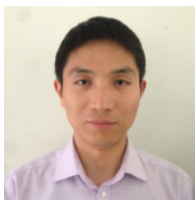
**Xiaotong Wu** received the Ph.D. degree in Computer Science and Technology from Nanjing University, China, in 2017. He is currently working as a lecturer in School of Computer and Electronic Information at Nanjing Normal University in China. His research interests include secure machine learning, big data privacy, federated learning.



**Qiang Ni** (M'04–SM'08) is currently a Professor and the Head of the Communication Systems Group, School of Computing and Communications, Lancaster University, Lancaster, U.K. His research interests include the area of future generation communications and networking, including green communications and networking, millimeter-wave wireless communications, cognitive radio network systems, non-orthogonal multiple access (NOMA), heterogeneous networks, 5G and 6G, SDN, cloud networks, energy harvesting, wireless information and power transfer, IoTs, cyber physical systems, AI and machine learning, big data analytics, and vehicular networks. He has authored or co-authored 300+ papers in these areas. He was an IEEE 802.11 Wireless Standard Working Group Voting Member and a contributor to various IEEE wireless standards.



**Yuan Yuan** is currently a Professor with the School of Computer Science and Engineering, Beihang University, China. He received the Ph.D. degree from the Department of Computer Science and Technology, Tsinghua University, Beijing, China, in 2015. From 2014 to 2015, he was a visiting Ph.D. student with the Centre of Excellence for Research in Computational Intelligence and Applications, University of Birmingham, U.K. He worked as a Research Fellow at the School of Computer Science and Engineering, Nanyang Technological University, Singapore, from 2015 to 2016. After then, He worked as a Postdoctoral Fellow with the Department of Computer Science and Engineering, Michigan State University, USA, from 2016 to 2021. His research interests include evolutionary computation, machine learning, and search-based software engineering.



**Xuyun Zhang** is currently working as a senior lecturer in School of Computing at Macquarie University in Australia. He worked as a lecturer in The University of Auckland during 2016 ~ 2019 and a postdoc researcher in NICTA during 2014 2016. His research interests include secure machine learning, big data privacy and cyber security.